Richter, C. (Ed.)
Proceedings of the Ocean Drilling Program, Scientific Results Volume 181

7. Microbial Sulfate Reduction in Interstitial Waters from Sediments of the Southwest Pacific (Sites 1119–1124): Evidence from Stable Sulfur Isotopes[1]

Michael E. Böttcher,[2] Boo-Keun Khim,[3] and Atsushi Suzuki[4]

ABSTRACT

Seventy-nine interstitial water samples from six sites (Ocean Drilling Program Sites 1119–1124) from the southwestern Pacific Ocean have been analyzed for stable isotopes of dissolved sulfate ($\delta^{34}S$), along with major and minor ions. Sulfate from the interstitial fluids ($\delta^{34}S$ values between +20.7‰ and +57.5‰ vs. the Vienna-Canyon Diablo troilite standard) was enriched in ^{34}S with respect to modern seawater ($\delta^{34}S \approx$ +20.6‰), indicating that differing amounts of microbial sulfate reduction took place at all investigated sites. Microbial sulfate reduction was found at all sites, the intensity depending on the availability of organic matter, which is controlled by paleosedimentation conditions (e.g., sedimentation rate and presence of turbidites). In addition, total reduced inorganic sulfur (essentially pyrite) as a product of microbial sulfate reduction was quantified in selected sediments from Site 1119.

INTRODUCTION

Interstitial waters from six Ocean Drilling Program (ODP) sites (Sites 1119–1124) from the southwestern Pacific Ocean (Fig. F1) were retrieved during Leg 181. Site 1119 (396 m water depth) was drilled close to the eastern shoreline of New Zealand's south island, Site 1120 (544 m

F1. Map of the southwestern Pacific with Leg 181 sampling sites, p. 8.

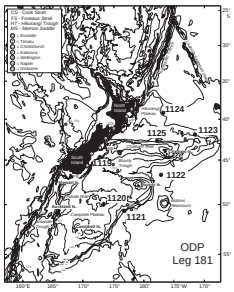

[1] Böttcher, M.E., Khim, B.-K., and Suzuki, A., 2002. Microbial sulfate reduction in interstitial waters from sediments of the southwest Pacific (Sites 1119–1124): evidence from stable sulfur isotopes. *In* Richter, C. (Ed.), *Proc. ODP, Sci. Results,* 181, 1–15 [Online]. Available from World Wide Web: <http://www-odp.tamu.edu/publications/181_SR/VOLUME/CHAPTERS/201.PDF>. [Cited YYYY-MM-DD]
[2] Department of Biogeochemistry, Max Planck Institute for Marine Microbiology, Celsiusstrasse 1, D-28359 Bremen, Germany. mboettch@mpi-bremen.de
[3] Polar Science Laboratory, KORDI, Ansan 425-600, Korea.
[4] Geological Survey of Japan, Ibaraki 305-8567, Japan.

Initial receipt: 5 February 2001
Acceptance: 19 September 2001
Web publication: 21 February 2002
Ms 181SR-201

water depth) is located on the shallow-water Campbell Plateau, and Site 1121 (4490 m water depth) on the Campbell "drift." Site 1122 (4432 m water depth) was drilled on the north flank of the abyssal Bounty Fan and Site 1123 (3290 m water depth) on the deep northeastern slopes of the Chatham Rise. Site 1124 (3957 m water depth) was positioned on the north-south–trending ridge of the Rekohu Drift (Fig. F1) (Carter, McCave, Richter, Carter, et al., 1999). Based on biostratigraphic criteria, sedimentation rates vary widely between 1.3 and 40 cm/k.y., and in composite, the recovered sediments span a time interval from the Late Cretaceous to the Holocene (Carter, McCave, Richter, Carter, et al., 1999).

Sulfur isotope signatures of dissolved sulfate in marine pore waters have been used as a valuable indicator for the occurrence of microbial sulfate reduction (e.g., Hartmann and Nielsen, 1969; Chanton et al., 1987; Böttcher et al., 2000). Despite the interest in the microbial activity of the deep biosphere (Parkes et al., 1994), only few studies have measured sulfur isotopes in pore waters of deep marine sediments (Zak et al., 1980; Brumsack et al., 1992; Böttcher et al., 1998, 1999; Rudnicki et al., 2001). In the present study, pore waters were retrieved from the six sites drilled during Leg 181 and analyzed for stable isotopes of dissolved sulfate ($^{34}S/^{32}S$), together with major and minor ions, as evidence for the activity of sulfate-reducing bacteria in the sediment–pore water system. Additionally, solid-phase total reduced inorganic sulfur ([TRIS] ≅ essentially pyrite + minor elemental sulfur + minor acid volatile sulfides), which originates from the sulfate reduction process, was measured in selected squeeze-cake samples from sediments of Site 1119.

SAMPLING AND ANALYTICAL METHODS

Interstitial water samples were squeezed from whole-round samples immediately after retrieval of the cores with the standard titanium-stainless steel ODP squeezer (Manheim and Sayles, 1974). The retrieved pore waters were subsequently analyzed on board the *JOIDES Resolution* for concentrations of major and minor constituents, including sulfate and chloride (Carter, McCave, Richter, Carter, et al., 1999), by using methods described by Gieskes et al. (1991). Sulfur isotope measurements of dissolved sulfate were performed on pore waters previously used for shipboard alkalinity determinations. The sulfate was precipitated quantitatively as $BaSO_4$ by the addition of a barium chloride solution, washed several times with deionized water, and dried at 110°C. Sulfur isotope ratios ($^{34}S/^{32}S$) were analyzed by combustion isotope ratio-monitoring mass spectrometry (Giesemann et al., 1994; Böttcher et al., 1998). After total conversion of barium sulfate to SO_2 via flash combustion in an elemental analyzer (Carlo Erba EA 1108), sample and standard gas were introduced into a Finnigan MAT 252 gas mass spectrometer via a Finnigan MAT Conflo II interface. Stable isotope ratios $^{34}S/^{32}S$ are given in the δ-notation with respect to the SO_2-based Vienna-Canyon-Diablo troilite (V-CDT) standard (Gonfiantini et al., 1995) according to ($R = {}^{34}S/{}^{32}S$):

$$\delta^{34}S(‰) = [R_{sample}/(R_{V\text{-}CDT} - 1)] \times 10^3.$$

Replicate measurements agreed within ±0.2‰. Solid-phase total reduced inorganic sulfur was extracted from selected dried squeeze-cake

sediments by hot distillation with acidic chromium(II)chloride solution (Canfield et al., 1986; Fossing and Jørgensen, 1989). This fraction includes sedimentary metal sulfides (essentially pyrite [FeS_2]) and minor primary elemental sulfur. Minor secondary sulfur may also have been formed as an oxidation product of acid-soluble iron sulfides during drying of the sediment samples.

RESULTS AND DISCUSSION

From the downward variation of dissolved sulfate concentrations in the interstitial waters (Fig. F2; Table T1), it is evident that all sites are characterized by more or less intense bacterial sulfate reduction throughout the sediment column. Sulfate reduction associated with the degradation of organic matter leads to the liberation of carbon dioxide, ammonium, and hydrogen sulfide (Froelich et al., 1979; Gieskes, 1981) according to the overall reaction

$$(CH_2O)_{106}(NH_3)_{16}(H_3PO_4) + 53SO_4^{2-} + 14H^+ \rightarrow 106HCO_3^- + 16NH_4^+ + HPO_4^{2-} + 53H_2S,$$

in general agreement with the observed downcore variations in sulfate, alkalinity, and ammonium (Fig. F3) (Carter, McCave, Richter, Carter, et al., 1999). Besides mineralization of organic matter, alkalinity data were additionally influenced by the carbonate diagenesis and sorption on clay minerals, respectively. Dissolved sulfate was completely exhausted within the first 20 m at Sites 1119 and 1122, indicating that rates of sulfate reduction exceed the supply rate of sulfate from the sediment/water interface. At Site 1123, most of the sulfate reduction seems to occur within the first 150 m of the sediment column. Low net sulfate reduction rates are found at Site 1120, 1121, and 1124.

Microbial reduction of dissolved sulfate causes a kinetic isotope effect. An enrichment of the lighter sulfur isotope ^{32}S in the formed hydrogen sulfide is the result (Kaplan and Rittenberg, 1964; Chambers and Trudinger, 1979), leading to a corresponding accumulation of the heavy isotope (^{34}S) in the residual sulfate (Hartmann and Nielsen, 1969; Jørgensen, 1979). Therefore, even at Site 1120 where the pore water sulfate concentrations only decrease slightly with depth (Fig. F2), microbial activities consuming sulfate as the electron acceptor are recorded by the sulfur isotopic composition of residual sulfate.

Reduction of dissolved sulfate in the sediment is coupled to the availability of metabolizable organic matter or hydrocarbons (mainly CH_4) (Berner 1980; Borowski et al. 1996; Hoehler et al., 1994; Boetius et al. 2000). In agreement with a controlling function of organic matter contents on the microbial activity, sulfate gradients are positively correlated to the bulk sedimentation rates (Carter, McCave, Richter, Carter, et al., 1999), which indicates higher preservation of metabolizable organic matter with an increasing sedimentation rate (Berner, 1980). The highest sedimentation rate is found in the upper parts of Sites 1119 and 1122 (Fig. F4), corresponding to a fast exhaustion of dissolved sulfate (Fig. F2). According to shipboard measurements, methane increased only where sulfate was completely depleted from the pore waters at Sites 1119 and 1122 (Carter, McCave, Richter, Carter, et al., 1999). In the zones of complete sulfate exhaustion at these sites, the dissolution of biogenic barite can be expected according to the concept of the de-

F2. Pore water sulfate and ^{34}S vs. depth, p. 9.

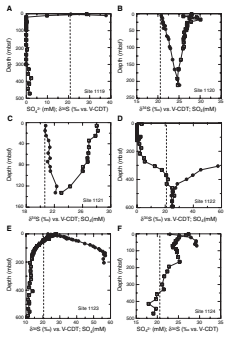

T1. Interstitial water composition, p. 13.

F3. Covariation of alkalinity and ammonium data with sulfate, p. 10.

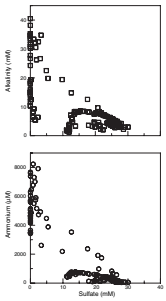

F4. Sedimentation rates for Sites 1119, 1120, 1122, 1123 and 1124, p. 11.

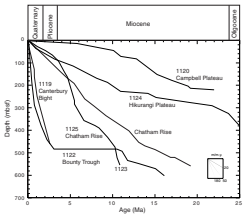

velopment of a diagenetic "barite fronts" (Brumsack et al., 1992; Torres et al., 1996). Following this model, diagenetic baryte formation may be initiated at the meeting points of upward-diffusing barium with downward-diffusing sulfate. Based on the isotopic composition of dissolved sulfate (~+60‰ vs. V-CDT), this diagenetic barite should be highly enriched in ^{34}S with respect to modern biogenic baryte (Paytan et al., 1998) and Pacific Ocean water sulfate (Longinelli, 1989; Böttcher et al., 2000).

The sulfate profiles at Sites 1119 and 1123 show a convex-up curvature (Fig. F2) which, together with the downward variations in alkalinity and dissolved ammonium (Carter, McCave, Richter, Carter, et al., 1999), indicate that sulfate reduction seems to be caused by in situ microbial degradation of organic matter and that upward diffusion of methane here plays no role in the upper part of the sedimentary column (Borowski et al., 1996).

Although sulfate reduction should be less significant in the deep sea when compared to continental shelf sediments (Jørgensen, 1982; Canfield, 1991), the highest net sulfate reduction was found at Site 1122 (4432 m water depth). However, below ~200 meters below seafloor (mbsf), sulfate started to increase again with depth and reached an apparent steady-state value below ~500 mbsf. The sulfur isotopic composition in the deep sediment layers decreased over this interval, but both parameters did not reach bottom-water conditions. This indicates that the deep pore waters had been influenced by microbial sulfate reduction. The dramatic change in the pore water composition in the deep sediment column corresponds to a change in the sedimentation rate from >40 cm/k.y. down to a rate of ~5 cm/k.y. (Fig. F3), which is substantiated by lithostratigraphic units and sedimentological properties. The upper 300 m of sediment consists of rhythmic upper Pleistocene sand turbidites and below 500 mbsf of upper Miocene current-influenced sands and muds. At ~260 mbsf, a high abundance of pyrite was observed at the base of the mud-wave sequence (Carter, McCave, Richter, Carter, et al., 1999), probably a result of enhanced microbial activity and/or some sorting phenomena during the turbidite settling processes. An unconformity exists at ~470–500 mbsf. The control of sulfate reduction by turbidites as carriers of reactive organic matter into the deep sea has been observed earlier in sediments of the deep Arabian Sea (~4040 m water depth) (Böttcher et al., 2000). Turbiditic sediments with enhanced organic carbon contents stimulated both microbial net (Böttcher et al., 2000) and gross (Boetius et al., 2000) sulfate reduction even in near-surface sediments.

TRIS contents measured at Site 1119 (Table T2) fit into the range of shipboard measurements of total sulfur; however, the TRIS data show no close covariaton with total organic carbon contents (Fig. F5). Under steady-state closed-system conditions, continuous increase of pyrite with depth until exhaustion of dissolved sulfate would be expected (Hartmann and Nielsen, 1969). Therefore, the strong fluctuations of TRIS contents in the sediment profile of Site 1119 probably indicate a dominant formation of pyrite close to the sediment/water interface (Berner, 1980) with some minor contributions from the zone of active net sulfate reduction.

In conclusion, sulfur isotope measurements on the dissolved sulfate of interstitial waters from the southwest Pacific clearly indicate the activity of sulfate reducing bacteria. Prime control for this process would be the delivery of metabolizable organic matter. This seems to be partly

T2. TRIS in squeeze-cake samples, p. 15.

F5. Downcore trends of TOC, TS, and TRIS, p. 12.

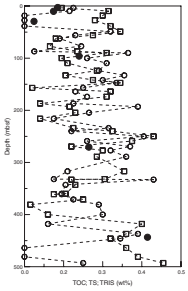

provided via turbidite sedimentation, as suggested by a coupling of high sedimentation rate and high sulfate turnover.

ACKNOWLEDGMENTS

We thank the scientific and technical crew of Leg 181 for support during sampling. The first author wishes to thank H.-J. Brumsack for inspiring discussions, J. Rullkötter for access to the gas mass spectrometer at the ICBM, J. Rinna for logistical support, and musical inspiration by E. Grieg and M. Knopfler during manuscript preparation. The manuscript was improved by reviews of H. Strauss and an anonymous reviewer. The second author (BKK) appreciates KODP for his participation on ODP Leg 181.

This research used samples and/or data provided by the Ocean Drilling Program (ODP). ODP is sponsored by the U.S. National Science Foundation (NSF) and participating countries under management of Joint Oceanographic Institutions (JOI), Inc. Funding for this research was provided by the Max Planck Society.

REFERENCES

Berner, R.A., 1980. *Early Diagenesis. A Theoretical Approach.* Princeton, NJ (Princeton Univ. Press).

Boetius, A., Ferdelman, T., and Lochte, K., 2000. Bacterial turnover of organic carbon of the deep Arabian Sea in relation to vertical flux. *Deep-Sea Res., Part II,* 47:1752–1783.

Borowski, W.S., Paull, C.K., and Ussler, W., III, 1996. Marine pore-water sulfate profiles indicate in situ methane flux from underlying gas hydrate. *Geology,* 24:655–658.

Böttcher, M.E., Bernasconi, S.M., and Brumsack, H.-J., 1999. Carbon, sulfur, and oxygen isotope geochemistry of interstitial waters from the western Mediterranean. *In* Zahn, R., Comas, M.C., and Klaus, A. (Eds.), *Proc. ODP, Sci. Results,* 161: College Station, TX (Ocean Drilling Program), 413–422.

Böttcher, M.E., Brumsack, H.-J., and De Lange, G.J., 1998. Sulfate reduction and related stable isotope (^{34}S, ^{18}O) variations in interstitial waters from the Eastern Mediterranean. *In* Robertson, A.H.F., Emeis, K.-C., Richter, C., and Camerlenghi, A. (Eds.), *Proc. ODP, Sci. Results,* 160: College Station, TX (Ocean Drilling Program), 365–373.

Böttcher, M.E., Schale, H., Schnetger, B., Wallmann, K., and Brumsack, H.-J., 2000. Stable sulfur isotopes indicate net sulfate reduction in near-surface sediments of the deep Arabian Sea. *Deep-Sea Res., Part II,* 47:2769–2783.

Brumsack, H.-J., Zuleger, E., Gohn, E., and Murray, R.W., 1992. Stable and radiogenic isotopes in pore waters from Leg 127, Japan Sea. *In* Pisciotto, K.A., Ingle, J.C., Jr., von Breymann, M.T., Barron, J., et al., *Proc. ODP, Sci. Results,* 127/128 (Pt. 1): College Station, TX (Ocean Drilling Program), 635–650.

Canfield, D.E., 1991. Sulfate reduction in deep-sea sediments. *Am. J. Sci.,* 291:177–188.

Canfield, D.E., Raiswell, R., Westrich, J.T., Reaves, C.M., and Berner, R.A., 1986. The use of chromium reduction in the analysis of reduced inorganic sulfur in sediments and shale. *Chem. Geol.,* 54:149–155.

Carter, R.M., McCave, I.N., Richter, C., Carter, L., et al., 1999. *Proc. ODP, Init. Repts.,* 181 [CD-ROM]. Available from: Ocean Drilling Program, Texas A&M University, College Station, TX 77845-9547, U.S.A.

Chambers, L.A., and Trudinger, P.A., 1979. Microbiological fractionation of stable sulfur isotopes: a review and critique. *Geomicrobiol. J.,* 1:249–293.

Chanton, J.P., Martens, C.S., and Goldhaber, M.B., 1987. Biogeochemical cycling in an organic-rich coastal marine basin, 8. A sulfur isotope budget balanced by differential diffusion across the sediment-water interface. *Geochim. Cosmochim. Acta,* 51:1201–1208.

Fossing, H. and Jørgensen, B.B., 1989. Measurement of bacterial sulfate reduction in sediments: evaluation of a single-step chromium reduction method. *Biogeochemistry,* 8: 205–222.

Froelich, P.N., Klinkhammer, G.P., Bender, M.L., Luedtke, N.A., Heath, G.R., Cullen, D., Dauphin, P., Hammond, D., Hartman, B., and Maynard, V., 1979. Early oxidation of organic matter in pelagic sediments of the eastern equatorial Atlantic: suboxic diagenesis. *Geochim. Cosmochim. Acta,* 43:1075–1090.

Giesemann, A., Jäger, H.-J., Norman, A.L., Krouse, H.R., and Brand, W.A., 1994. Online sulphur isotope determination using an elemental analyzer coupled to a mass spectrometer. *Anal. Chem.,* 66:2816–2819.

Gieskes, J., Gamo, T., and Brumsack, H.-J., 1991. Chemical methods for interstitial water analysis aboard *JOIDES Resolution. ODP Tech. Note,* 15.

Gieskes, J.M., 1981. Deep sea drilling interstitial water studies: implications for chemical alteration of the oceanic crust, layers I and II. *In* Warme, J.E., Douglas, R.G. and

Winterer, E.L. (Eds.), *The Deep Sea Drilling Project: A decade of progress*. Spec. Publ.—Soc. Econ. Paleontol. Mineral., 32:149–167.

Gonfiantini, R., Stichler, W., and Rozanski, K., 1995. Standards and intercomparison materials distributed by the International Atomic Energy Agency for stable isotope measurements. *IAEA-TECDOC*-825, 13–29.

Hartmann, M., and Nielsen, H., 1969. δ^{34}S-Werte in rezenten Meeressedimenten und ihre Deutung am Beispiel einiger Sedimentprofile aus der westlichen Ostsee. *Geol. Rundsch.,* 58:621–655.

Hoehler, T.M., Alperin, M.J., Albert, D.B., and Martens, C.S., 1994. Field and laboratory studies of methane oxidation in anoxic marine sediment: evidence for a methanogen-sulfate reducer consortium. *Global Biogeochem. Cycles,* 8:451–463.

Jørgensen, B.B., 1979. A theoretical model of the stable sulfur isotope distribution in marine sediments. *Geochim. Cosmochim. Acta,* 31:363–374.

————, 1982. Mineralization of organic matter in the seabed—the role of sulphate reduction. *Nature,* 296:643–645.

Kaplan, I.R. and Rittenberg, S.C., 1964. Microbiological fractionation of sulphur isotopes. *J. Gen. Microbiol.,* 34:195–212.

Longinelli, A., 1989. Oxygen-18 and sulphur-34 in dissolved oceanic sulphate and phosphate. *In* Fritz, P., and Fontes, J.C. (Eds.), *Handbook of Environmental Isotope Geochemistry* (Vol. 3): New York (Elsevier), 219–256.

Manheim, F.T., and Sayles, F.L., 1974. Composition and origin of interstitial waters of marine sediments, based on deep sea drill cores. *In* Goldberg, E.D. (Ed.), *The Sea* (Vol. 5): *Marine Chemistry: The Sedimentary Cycle:* New York (Wiley), 527–568.

Parkes, R.J., Cragg, B.A., Bale, S.J., Getliff, J.M., Goodman, K., Rochelle, P.A., Fry, J.C., Weightman, A.J., and Harvey, S.M., 1994. Deep bacterial biosphere in Pacific Ocean sediments. *Nature,* 371: 410–413.

Paytan, A., Kastner, M., Campbell, D., and Thiemens, M.H., 1998. Sulfur isotopic composition of Cenozoic seawater sulfate. *Science,* 282:1459–1462.

Rudnicki, M.D., Elderfield, H., and Spiro, B., 2001. Fractionation of sulfur isotopes during bacterial sulfate reduction in deep ocean sediments at elevated temperatures. *Geochim. Cosmochim. Acta,* 65:777–789.

Torres, M.E., Brumsack, H.-J., Bohrmann, G., and Emeis, K.C., 1996. Barite fronts in continental margin sediments: a new look at barium remobilization in the zone of sulfate reduction and formation of heavy barites in diagenetic fronts. *Chem. Geol.,* 127:125–139.

Zak, I., Sakai, H., and Kaplan, I.R., 1980. Factors controlling the $^{18}O/^{16}O$ and $^{34}S/^{32}S$ isotope ratios of ocean sulfates, evaporites and interstitial sulfates from modern deep sea sediments. *In* Goldberg, E.D., Horibe, Y., and Saruhashi, K. (Eds.), *Isotope Marine Chemistry:* Tokyo (Rokakuho), 339–373.

Figure F1. Outline map of the southwestern Pacific with Leg 181 sampling sites (modified after Carter, McCave, Richter, Carter, et al., 1999).

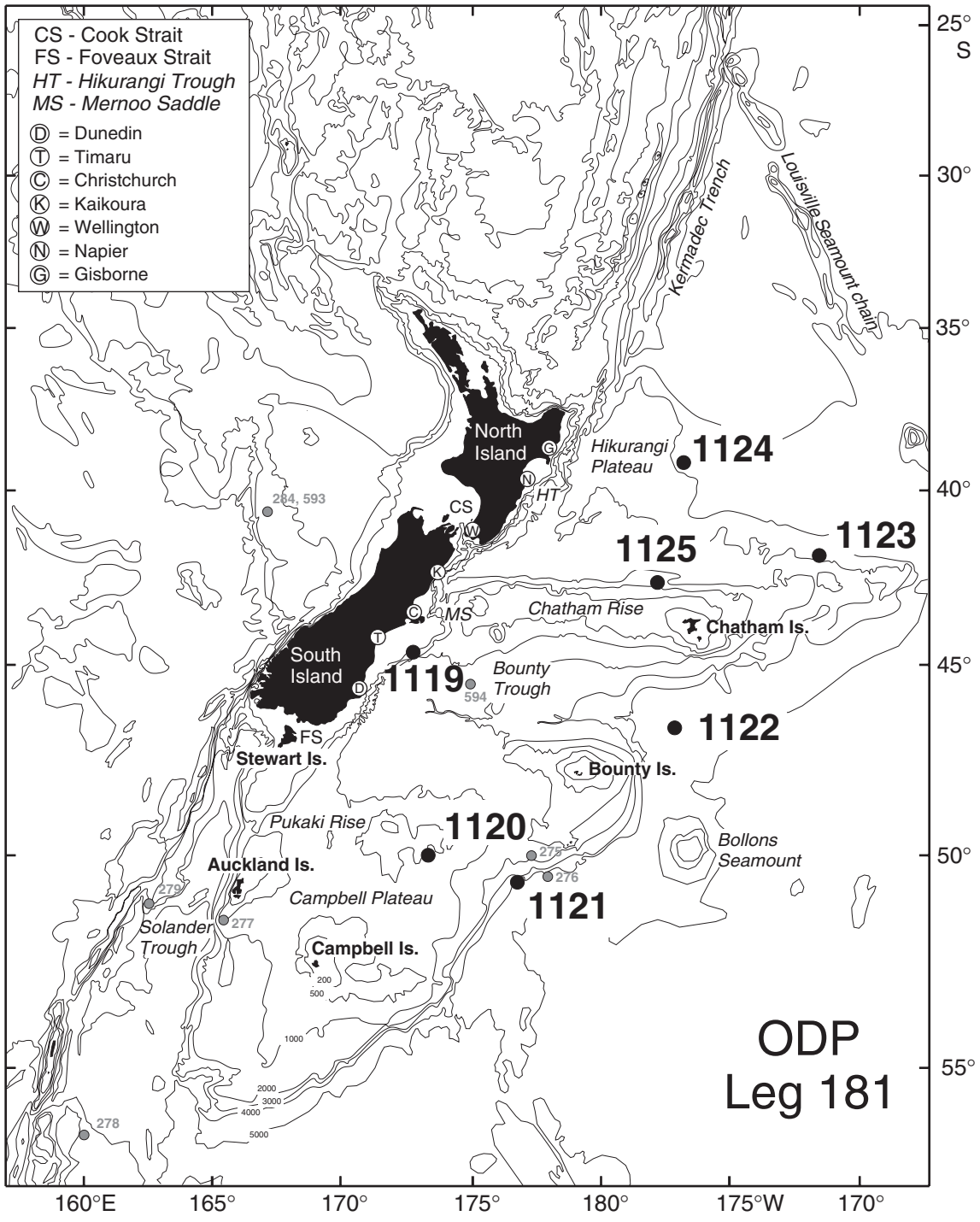

Figure F2. Pore water sulfate concentration (open symbols) and ^{34}S data (closed symbols) vs. depth profiles for Sites 1119–1124 (see Table T1, p. 13). V-CDT = Vienna-Canyon Diablo troilite standard.

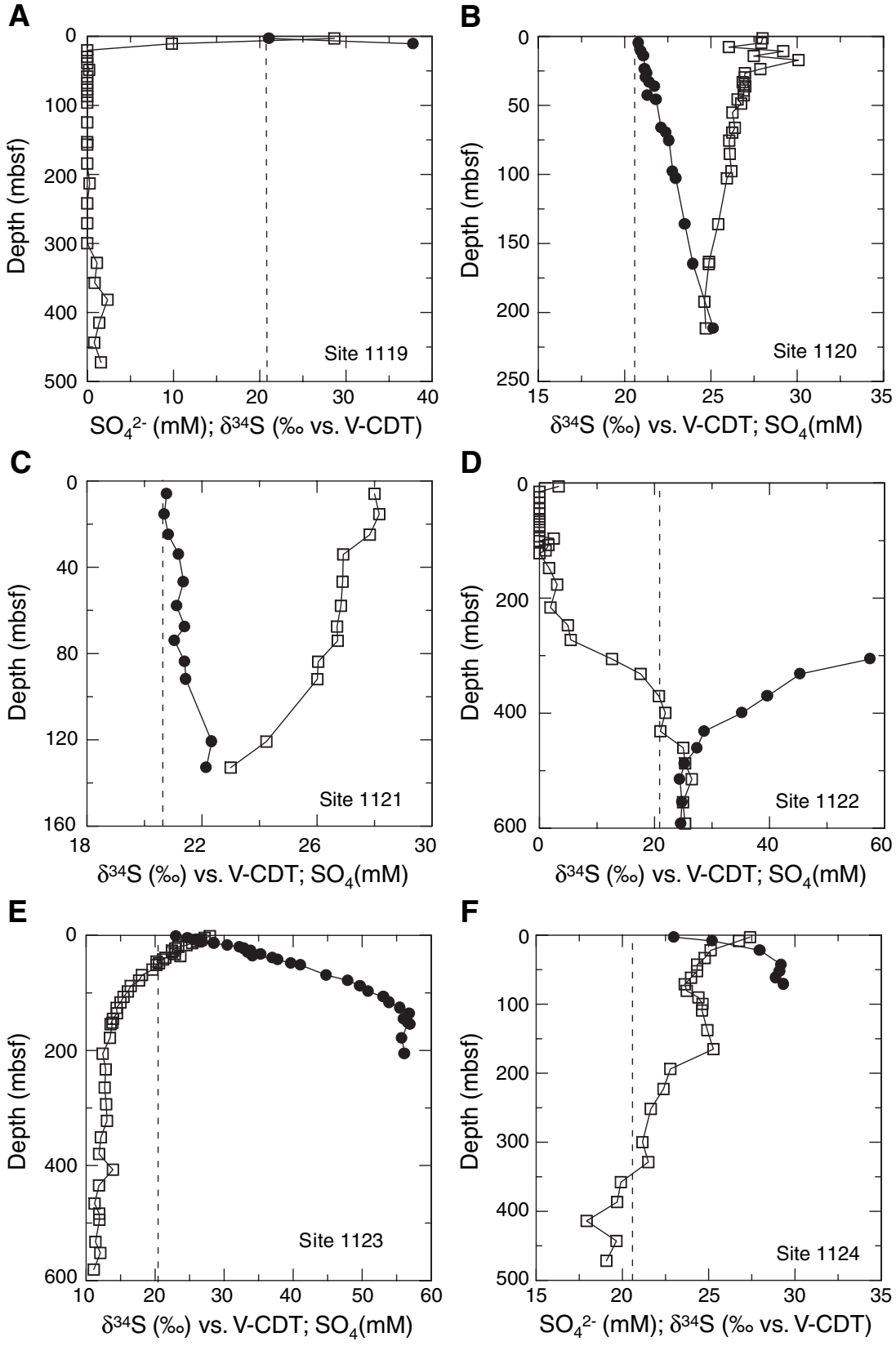

Figure F3. Covariation of alkalinity and ammonium data with sulfate at Sites 1119–1124 (data from Carter, McCave, Richter, Carter, et al., 1999).

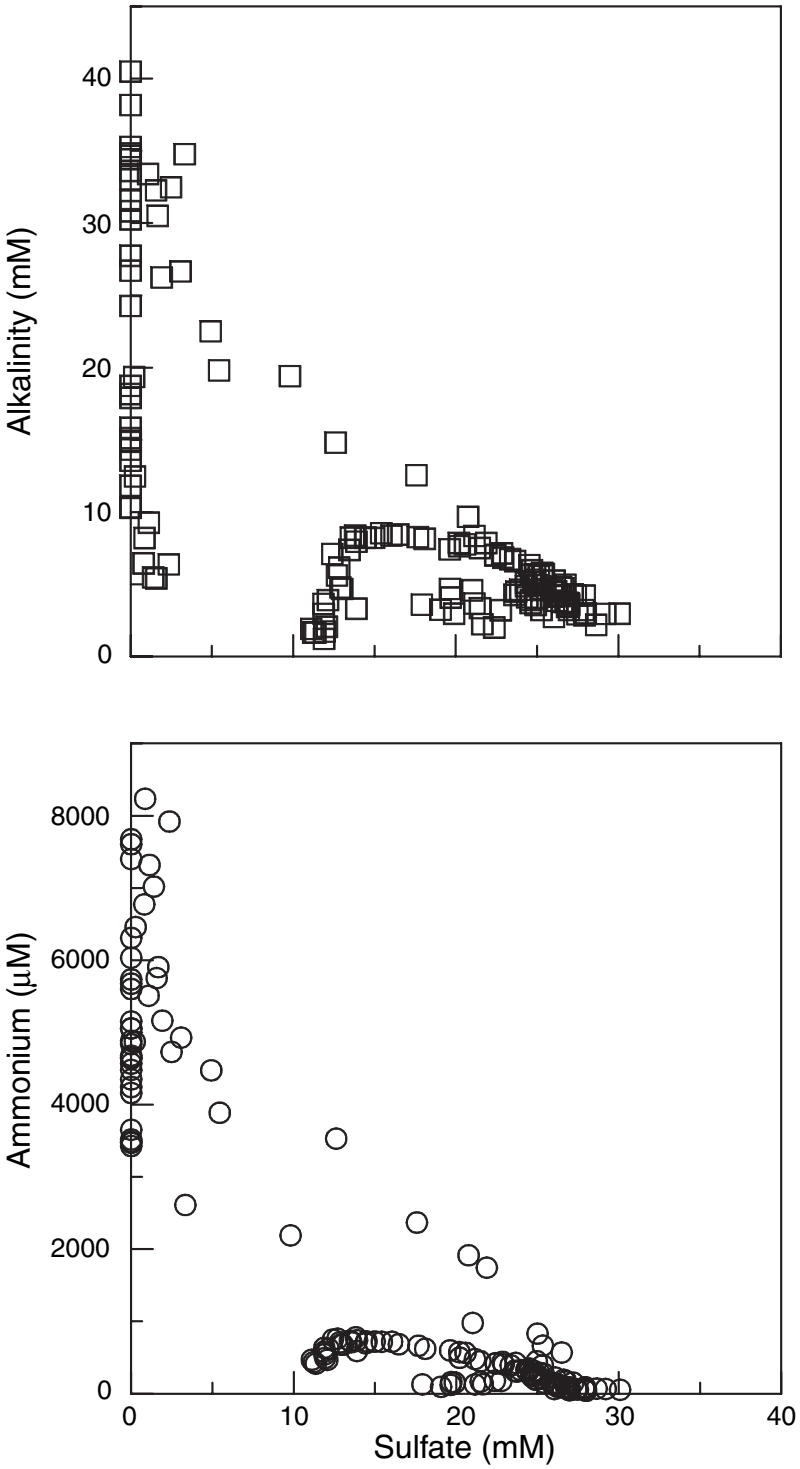

Figure F4. Sedimentation rates for Sites 1119, 1120, 1122, 1123 and 1124 (modified after Carter, McCave, Richter, Carter, et al., 1999).

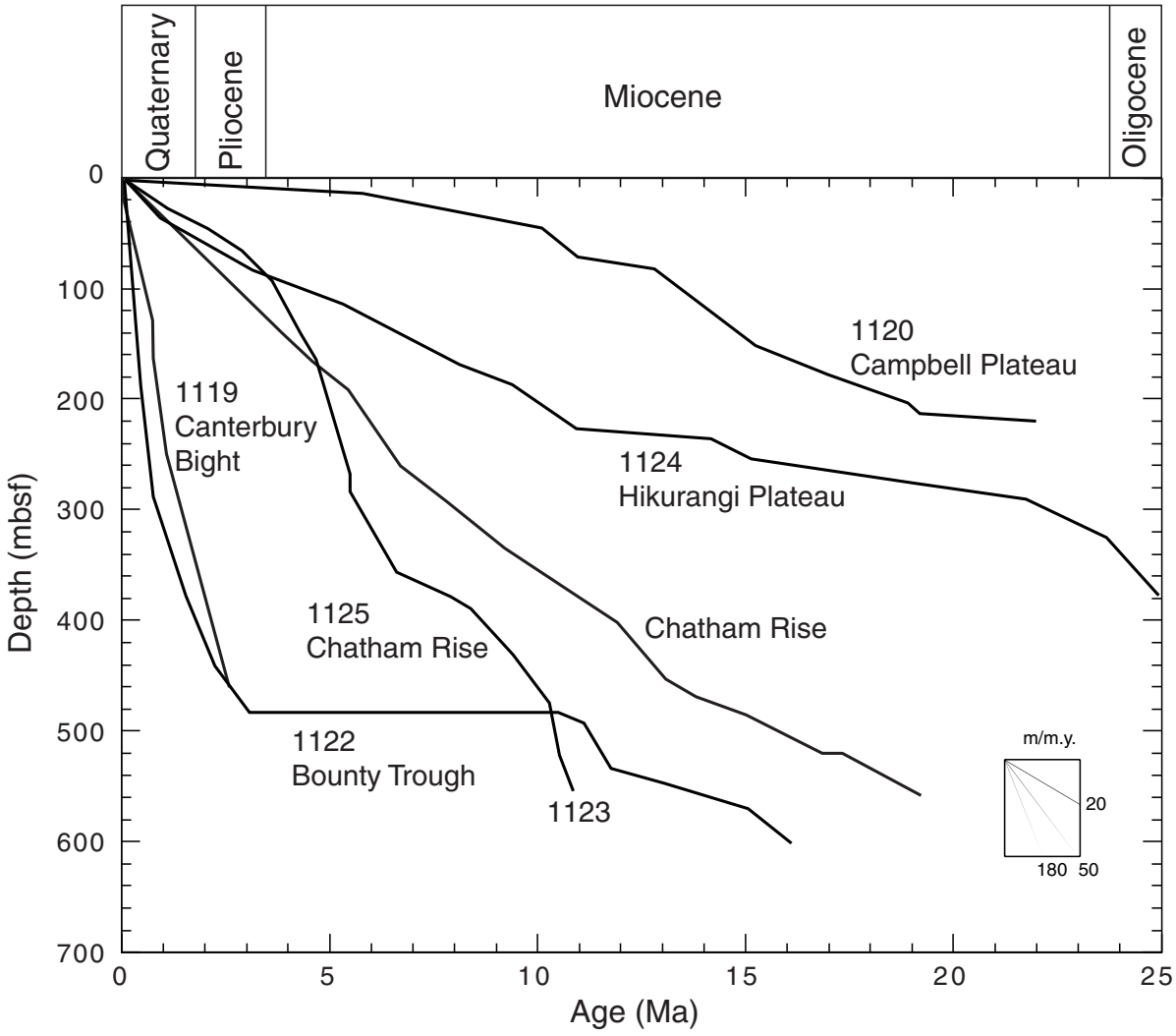

Figure F5. Downcore trends of total organic carbon ([TOC] open squares), total sulfur ([TS] open circles), and TRIS (closed circles) at Site 1119. TOC and TS data are from Carter, McCave, Richter, Carter, et al. (1999).

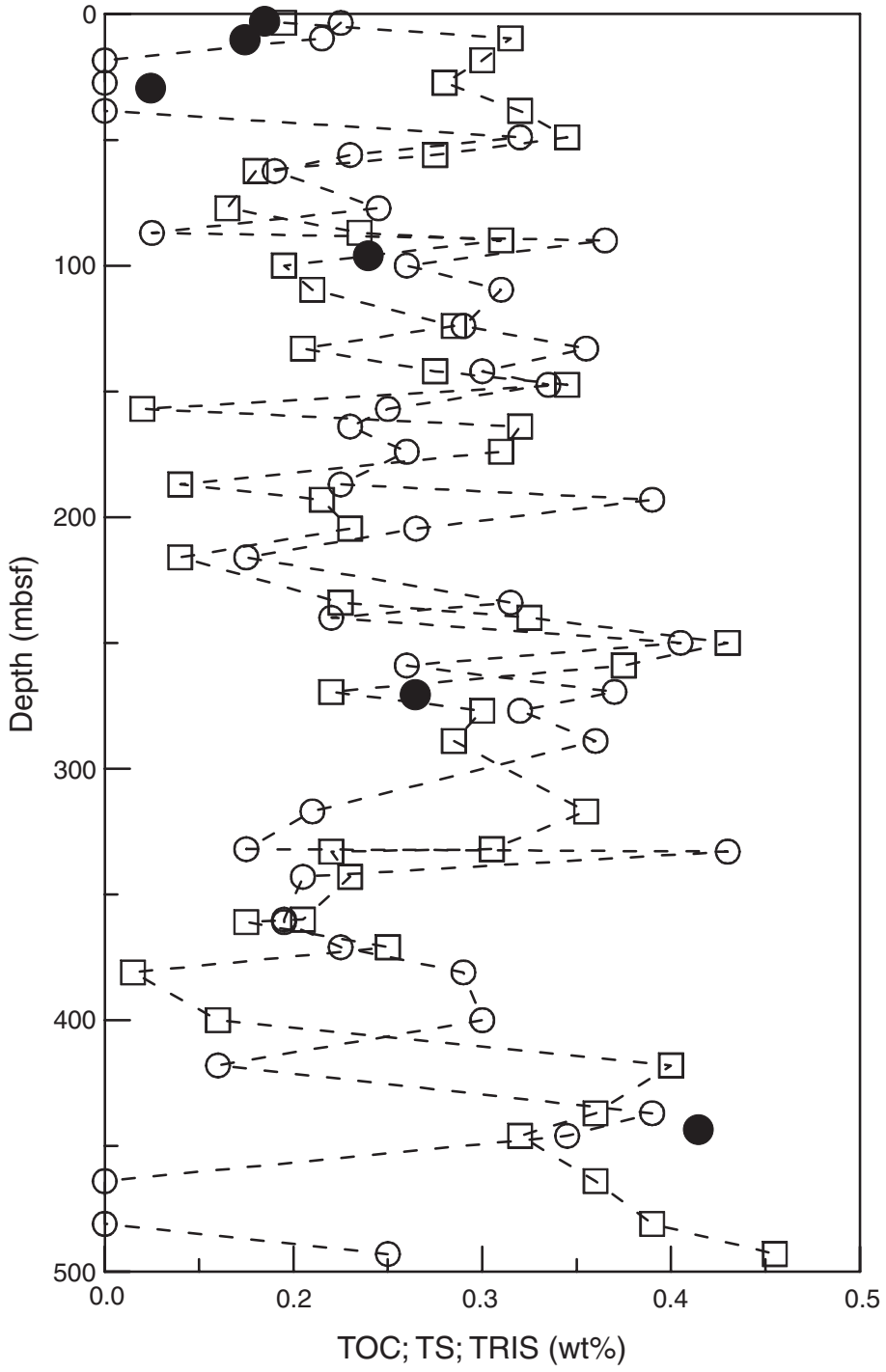

Table T1. Chloride and sulfate concentrations and stable sulfur isotope ratios in sulfate of interstitial waters from Leg 181. (See table notes. Continued on next page.)

Core, section, interval (cm)	Depth (mbsf)	Cl^- (mM)	SO_4^{2-} (mM)	$\delta^{34}S$ (‰)
181-1119B-				
1H-2, 145–150	2.95	552	28.6	+21.1
2H-4, 145–150	10.6	555	39.8	+37.8
3H-4, 145–150	20.15	551	0.0	ND
4H-4, 135–140	29.65	550	0.0	ND
5H-4, 135–140	39.05	549	0.0	ND
6H-4, 145–150	48.65	549	0.2	ND
7H-4, 135–140	58.05	547	0.0	ND
8H-4, 140–155	67.60	548	0.0	ND
9H-4, 135–140	77.05	545	0.0	ND
10H-4, 140–50	86.60	548	0.0	ND
11H-4, 140–150	96.10	547	0.0	ND
14H-4, 150–155	124.70	551	0.0	ND
17H-4, 140–150	153.10	550	0.0	ND
181-1119C-				
17H-4, 140–150	156.70	551	0.0	ND
20X-4, 140–150	184.20	550	0.0	ND
23X-4, 140–150	213.10	555	0.3	ND
26X-4, 140–150	241.90	552	0.0	ND
29X-4, 140–150	270.70	556	0.0	ND
32X-4, 140–150	299.70	556	0.0	ND
35X-4, 140–150	328.20	558	1.1	ND
38X-4, 140–150	357.00	557	0.9	ND
41X-1, 140–150	381.50	559	2.4	ND
44X-4, 140–150	414.90	558	1.4	ND
47X-4, 140–150	443.80	560	0.8	ND
50X-4, 140–150	472.30	562	1.6	
181-1120B-				
1H-1, 145–150	1.45	550	28.0	ND
2H-1, 145–150	4.75	549	27.9	+20.8
2H-1, 145–150	7.75	550	26.0	ND
2H-5, 145–150	10.75	551	29.2	+20.9
3H-1, 145–150	14.25	551	27.5	+21.1
3H-3, 135–140	17.15	551	30.1	ND
4H-1, 140–150	23.70	555	27.9	+21.2
4H-3, 135–145	26.65	550	27.0	+21.3
4H-5, 140–150	29.70	552	27.0	+21.2
5H-1, 140–150	33.20	552	26.8	+21.4
5H-3, 140–150	36.20	555	27.0	+21.7
5H-5, 140–150	39.20	555	26.9	ND
6H-1 140–150	42.70	554	26.9	+21.3
6H-3, 140–150	45.70	555	26.5	+21.8
6H-5, 140–150	48.70	555	26.8	ND
7H-3, 140–150	55.20	554	26.3	ND
8H-4, 140–150	66.20	557	26.4	+22.1
9X-1, 140–150	69.70	556	26.2	+22.4
11X-2, 140–150	75.50	556	26.1	+22.6
11X-2, 140–150	85.10	557	26.1	ND
12X-4, 140–150	97.70	557	26.2	+22.8
13X-1, 140–150	102.80	557	25.9	+23.0
16X-4, 140–150	136.00	558	25.4	+23.5
19X-4, 140–150	164.90	560	24.9	+24.0
181-1120D-				
1X-4, 140–150	163.30	564	24.9	ND
4X-4, 140–150	192.20	563	24.6	ND
7X-1, 140–150	211.50	561	24.7	+25.2
181-1121B-				
1H-4, 145–150	5.95	554	28.0	20.8
2H-4, 140–150	15.40	565	28.2	20.7
3H-4, 140–150	24.90	562	27.8	20.8
6X-1, 140–150	34.10	562	26.9	21.2
7X-3, 140–150	46.70	562	26.9	21.4
8X-4, 140–150	57.90	563	26.8	21.1
9X-4, 140–150	67.50	562	26.7	21.4
10X-4, 140–150	74.10	562	26.7	21.1
11X-2, 140–150	83.80	564	26.0	21.4
12X-1, 140–150	91.90	561	26.0	21.4
15X-1, 140–150	120.80	557	24.2	22.3
17X-2, 140–150	132.90	549	23.0	22.2
181-1122A-				
1H-4, 140–150	5.90	560	3.3	ND
2H-4, 140–150	15.20	562	0.0	ND
3H-4, 140–150	24.70	562	0.0	ND
4H-4, 140–150	34.20	563	0.0	ND
5H-5, 130–140	45.10	561	0.0	ND
6H-4, 140–150	53.20	560	0.0	ND
7H-4, 140–150	62.70	557	0.0	ND
9H-4, 140–150	67.40	560	0.0	ND
10H-4, 140–150	76.90	559	0.0	ND
12H-4, 140–150	92.80	556	0.0	ND
11X-1, 140–150	96.40	553	2.5	ND
13H-4, 140–150	100.80	556	0.0	ND
12X-2, 140–150	107.60	553	1.6	ND
13X-2, 140–150	117.20	553	1.1	ND
16X-3, 140–150	122.00	554	0.0	ND
19X-1, 140–150	147.90	554	1.7	ND
22X-1, 130–140	176.60	556	3.1	ND
26X-2, 90–100	216.40	556	1.9	ND
29X-3, 140–150	247.30	556	4.9	ND
32X-1, 140–150	272.70	555	5.4	49.3
35X-4, 140–150	305.90	557	12.6	57.5
38X-2, 140–150	331.80	556	17.6	45.4
42X-2, 140–150	370.40	559	20.8	39.6
45X-2, 140–150	399.50	559	21.9	35.2
48X-4, 140–150	431.40	557	21.0	28.7
51X-4, 140–150	460.30	559	25.0	27.4
54X-3, 140–150	487.40	557	25.3	25.2
57X-2, 140–150	514.80	557	26.5	24.4
61X-3, 140–150	554.80	557	25.0	24.8
65X-2, 140–150	591.80	556	25.3	24.6
181-1123A-				
1H-1, 140–150	1.40	555	27.9	23.0
1H-3, 135–145	4.35	556	27.2	24.7
2H-1, 140–150	7.50	556	26.6	25.7
2H-3, 140–150	10.50	557	26.1	26.8
2H-5, 140–150	13.50	558	25.4	28.5
3H-1, 140–150	17.00	559	24.5	30.5
3H-3, 140–150	20.00	561	23.3	32.2
3H-5, 120–130	22.80	561	22.9	32.9
4H-1, 140–150	26.50	562	22.4	33.9
4H-3, 140–150	29.50	563	22.4	33.5
4H-5, 140–150	32.50	563	22.9	35.3
5H-1, 140–150	36.00	562	23.7	34.2
5H-3, 140–150	39.00	562	21.5	37.0
5H-5, 140–150	42.00	562	21.2	37.8
6H-1, 140–150	45.50	562	20.2	ND
6H-3, 140–150	48.50	562	20.6	39.7
6H-5, 140–150	51.50	563	20.2	41.1
7H-4, 140–150	59.50	563	19.6	ND
8H-4, 140–150	69.00	564	18.1	44.8
9H-4, 140-150	78.50	563	17.7	48.0
10H-4, 140–150	88.00	563	16.5	49.7
11H-4, 140–150	97.50	564	16.1	50.9
12H-4, 140–150	107.00	564	15.4	53.1
13H-4, 140–150	116.50	564	15.0	53.9
14H-4, 140–150	126.00	564	14.4	55.5
15H-4, 140–150	135.50	564	14.5	56.8
16H-4, 140–150	145.00	564	13.9	56.1
17H-4, 140–150	154.50	563	13.5	57.0
181-1123B-				
17H-4, 140–150	151.80	564	13.8	56.7
20X-4, 140–150	178.20	565	13.5	55.8
23X-3, 140–150	205.60	564	12.4	56.1

Table T1 (continued).

Core, section, interval (cm)	Depth (mbsf)	Cl^- (mM)	SO_4^{2-} (mM)	$\delta^{34}S$ (‰)
26X-2, 140–150	232.90	567	12.8	ND
29X-4, 140–150	264.70	565	12.7	ND
32X-4, 140–150	293.60	566	12.9	ND
35X-4, 140–150	322.40	563	13.0	ND
38X-4, 140–150	351.00	565	12.1	ND
41X-4, 140–150	380.00	564	11.9	ND
44X-3, 135–150	407.35	565	13.9	ND
47X-2, 135–150	434.65	565	11.9	ND
50X-4, 135–150	466.25	559	11.2	ND
52X-3, 135–150	483.65	561	11.9	ND
181-1123C-				
19X-4, 135–150	494.4	573	11.9	ND
22X-4, 135–150	532.9	574	11.4	ND
25X-4, 135–150	552.1	576	12.1	ND
28X-4, 135–150	581.0	578	11.1	ND
31X-4, 135–150	609.8	573	11.7	ND
33X-1, 123–135	624.4	ND	ND	ND

Notes: Chloride and sulfate data from Carter, McCave, Richter, Carter, et al. (1999). ND = not determined.

Table T2. Contents of total reduced inorganic sulfur (TRIS) in squeeze cake samples, Site 1119.

Core, section, interval (cm)	Depth (mbsf)	TRIS (wt%)
181-1119B-		
1H-2, 145–150	2.95	0.17
2H-4, 145–150	10.65	0.15
4H-4, 135–140	29.65	0.05
11H-4, 140–150	96.10	0.28
181-1119C-		
29X-4, 140–150	270.70	0.33
47X-4, 140–150	443.80	0.63